

ESTIMATING WATER STORAGE IN RESERVOIRS  
BY SATELLITE OBSERVATIONS AND DIGITAL ELEVATION MODEL  
- A CASE STUDY OF THE YAGISAWA RESERVOIR -

By

Jun MAGOME

Graduate Student, Yamanashi University, Kofu, Yamanashi, Japan

Kuniyoshi TAKEUCHI

Graduate School of Engineering, Yamanashi University, Kofu, Yamanashi, Japan

and

Hiroshi ISHIDAIRA

Graduate School of Engineering, Yamanashi University, Kofu, Yamanashi, Japan

SYNOPSIS

Monitoring the spatial and temporal distribution of water storage in reservoirs is important for water resources management as well as for research on water cycle on a global scale. In this study, a new method of estimating water storage in a reservoir is proposed based on satellite observations and on a Digital Elevation Model (DEM). The relationship between the area of water surface ( $A$ ) and the volume of water storage ( $V$ ) is calculated from a DEM, and expressed as  $V=aA^b$ . By using this relation, the water surface measured from satellite images can be transformed into the volume of water storage. The method proposed is applied to the Yagisawa-reservoir, which is located in the upper reach of the Tone River basin in Japan. Although the accuracy of estimated water storage is not necessarily satisfactory and yet to be much improved, the possibility of estimating storage volume by this method is well demonstrated in this paper.

INTRODUCTION

Increasing water demand due to dramatic growth of population is one of the most serious problems in the 21<sup>st</sup> century. The amount of water on the Earth is limited, and part of water is becoming unusable because of water pollution. Therefore, we need to monitor water resources availability for their efficient and sustainable use. Currently river water, ground water and water in reservoirs are used for water supply for municipal, agricultural, and industrial purposes, which meet most of our water demands. Thus the monitoring of water storage in reservoirs is very important for managing water resources.

Although reservoirs are so important in water resources development and management, the influence of reservoirs on water cycles on a continental or global scale, due to impoundment and runoff delay, has been identified increasingly serious in recent studies (e.g. Vorosmatry et al. (1)). The International Commission on Large Dams (2)(3) reports that more than 41,413 dams over the height of 15m are now in operation, and increased by 688% from 1950 to 1986. These impoundments provided many important benefits to society such as flood control, hydroelectricity, and water storage for agriculture, industry, and municipalities. On the

other hand, these impoundments affect water cycles by increasing residence time of river water, which cause many problems, that is, the siltation of reservoirs, scouring of channels downstream, and the interference with the migration and habitats of aquatic organisms. Vorosmatry et al. (1) investigated the global distribution of residence time of river water by using global drainage networks with 30-minute spatial resolution and storage capacity data larger than  $0.5 \text{ km}^3$  of large reservoirs. In that study, they found that the delay of runoff induced by reservoirs would be larger than 3 months at the mouth of several large rivers. Therefore, continuous monitoring of water storage in reservoirs on large scale is very important to evaluate the influence of impoundments of reservoirs for water cycle on the earth.

To monitor water storage in reservoirs over a large area, a remote sensing technique can be a useful tool. A number of studies have been made on the monitoring of land surface hydrological condition by using satellite remote sensing, including detection of water surface (e.g. Rikimaru et al. (4), Mutuda et al. (5)). It is possible to understand the tendency of water storage changes in reservoirs by monitoring the expansion or contraction of the area of water surface. However, the remote sensing for land surface can only provide plane information such as the area of water surface, and the volume of water storage cannot be observed directly. Therefore, a method of transforming the area of water surface, which is obtained through remote sensing, into the volume of water storage should be investigated.

In this study, we propose a new method of estimating water storage in reservoirs based on satellite observations and digitized topography data. In the method proposed, the area of water surface (A) measured from satellite images is transformed into the volume of water storage (V) by using the relationship between the area of water surface (A) and the volume of water storage (V) (called as "*A-V relation*") derived from Digital Elevation Model (DEM). The proposed method is applied to the Yagisawa-reservoir in Japan to verify the possibility of estimating the water storage in reservoirs.

## STUDY AREA AND DATA

### Study area

The study area is the Yagisawa-reservoir, located in the upper reach of the Tone River basin in northern Gunma, Japan (Fig.1). In order to supply water for the Metropolitan area, many dams were constructed in the upper Tone River basin, and the Yagisawa-dam is one of the major multi-purpose dams in Japan. The gross storage capacity of the reservoir is 243 million  $\text{m}^3$  and the area of water surface for the high water level of flood is  $5.674 \text{ km}^2$ . The dam site is located in a deep valley surrounded by steep topography.

### Satellite images

Various satellite data are currently being collected and used for hydrological applications. In this study, satellite images derived from three different sensors are used to obtain the area of water surface, that is,

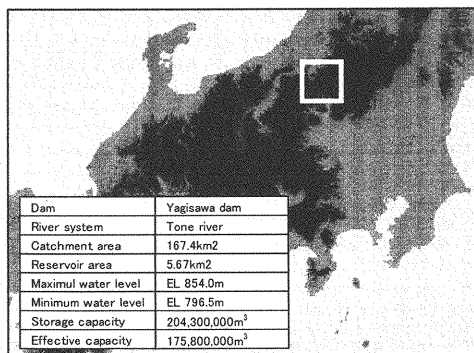


Fig.1 Location of the study site (Yagisawa-reservoir)

Table1 Specifications of sensors and images

satellite sensor	band	wavelength	resolution	area
SPOT HRV-XS	1	0.50~0.59 $\mu\text{m}$	20m	60km
	2	0.61~0.68 $\mu\text{m}$	20m	x
	3	0.79~0.89 $\mu\text{m}$	20m	60km
ADEOS AVNIR-M	1	0.42~0.50 $\mu\text{m}$	16m	80km
	2	0.52~0.60 $\mu\text{m}$	16m	x
	3	0.61~0.69 $\mu\text{m}$	16m	80km
	4	0.76~0.89 $\mu\text{m}$	16m	
J-ERS1 SAR		23.5 cm (1.275Ghz)	12.5m	75km x 75km

Synthetic Aperture Radar (SAR) images from JERS-1/SAR, Visible and Near Infrared images of SPOT/HRV-XS and ADEOS/AVNIR-M. The specifications of each sensor are listed in Table 1.

a) Visible and Near Infrared images

The multi-spectral images of visible and near infrared bands can provide details of specific earth features such as vegetation and water. However, the land surface condition below clouds cannot be observed. The cloud-free images of the study area are searched from satellite image archive of National Space Development Agency of Japan (NASDA) and following 7 scenes are selected, 6 scenes of SPOT/HRV-XS images were obtained from Aug. 8, 1994 to Jun. 1, 1998, and an ADEOS/AVNIR-M image on Jan. 16, 1997.

b) SAR images

JERS-1/SAR provides image of an area of 75km x 75km with high spatial resolution (12.5m). Since the microwave penetrates clouds, SAR can be used for detection of signal from land surface even in cloudy conditions. Therefore, it is suitable for the continuous monitoring of land surface conditions. Twelve scenes of JERS-1/SAR images collected from Aug. 8, 1994 to Jun. 1, 1998 are used in this study.

## DEM

In order to identify the A-V relation of the reservoir accurately, fine resolution DEM is required. In this study, the "Digital Map 50m Grid (Elevation)" issued by Geographical Survey Institute, Japan is used as DEM. It has the finest resolution of available DEMs in Japan. The data are collected with 1.5 x 2.25-arc-second spacing in latitude and longitude (approximately 50m x 50m), and the vertical resolution of the data is one meter.

## REPRESENTATION OF THE A-V RELATION

### A-V relation

Takeuchi (6)(7) showed that the A-V relation can be expressed as eq.(1) for reservoir in a valley topography with a "open book shape", as shown in Fig.2, where the shape of cross section is described as  $h = \alpha x^\beta$  ( $h$ : elevation,  $x$ : distance from the center of the valley,  $\alpha, \beta$ : parameters), and the longitudinal gradient of the valley ( $\theta$ ) is assumed as the constant;

$$V = a \cdot A^b \quad (1)$$

where  $V$ : volume of water storage,  $A$ : area of water surface;  $a, b$ : parameters in A-V relation;

$$a = \frac{\theta(\beta+1)}{2(\beta+1)} \cdot \frac{2\alpha\beta}{\theta(\beta+1)} \cdot \frac{1}{\beta+1} \quad (2)$$

$$b = \frac{1}{\beta+1} \quad (3)$$

If the shape of cross section is expressed as  $h = \alpha x$  ( $\beta=1$ ),  $V$  would be proportional to  $A^{1.5}$  because of geometrical similarity. The average A-V relation in the world (Fig.3) is obtained as eq.(4) by using the pair data of  $A$  and  $V$  (for high water level) from 7,936 reservoirs in the world, which can be founded in the World Register of Dams (2) and Yearbook of Dams (8) (Takeuchi (6)(7)).

$$V = 9.208 \cdot A^{1.114} \quad (A: \text{km}^2, V: 10^6 \text{m}^3) \quad (4)$$

Based on previous studies, eq.(1) is applied to represent A-V relation of a reservoir.

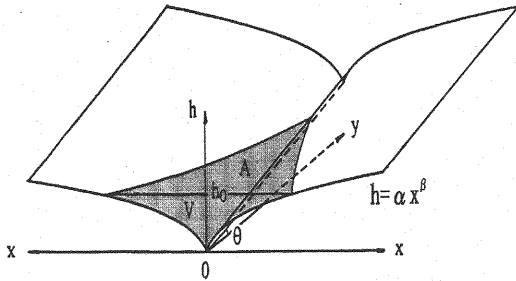


**Fig.2** A hypothetical valley with cross-section  $h = \alpha x^\beta$  and gradient  $\theta$  (Takeuchi 1998)

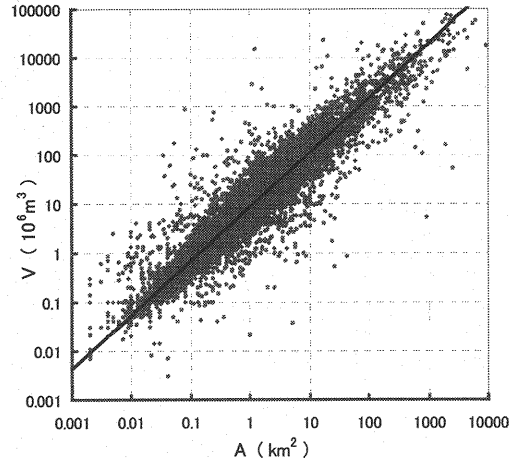


**Fig.3** The average A-V relation in the world (Takeuchi 1997,1998)

#### Parameter identification for A-V relation

##### a) Calculation of the area of water surface (A) and the volume of water storage (V)

The area of water surface (A) and the volume of water storage (V) of a reservoir under arbitrary water level are calculated from grid base DEM by means of the following procedure (Magome et al. (9)):

- i) Searching the grid cells which have lower elevation than the water level.
- ii) Grouping the grid cells of i). Each group consists of the grid cells that are continuously linked each other.
- iii) The group, which is located in the upstream of dam site and adjacent to the dam, is assumed as grid cells in the reservoir. These grid cells are called as “reservoir grids”(Fig.4).
- iv) The reservoir is expressed as an aggregate of rectangular parallelepipeds in the reservoir grids (Fig.5), where the height of each parallelepiped is estimated as the difference between the water level and elevation of each grid cell. A is calculated by multiplying the numbers of reservoir grids and the area of a grid, and V is obtained as the sum of the volume of rectangular parallelepipeds for all reservoir grids.

The above-mentioned procedure is applied repeatedly for each water level that starts from the ground level of the dam site to several ten meters with an interval of 1 meter. Then, continuous A and V for several water levels are calculated.

##### b) Correction of estimated volume of water storage (V)

Some of dams in Japan were constructed before the DEM (the “*Digital Map 50m Grid (Elevation)*”) was established. As for these dams, the reservoir grids are filled with a constant elevation of water surface, and the natural topography under the water surface cannot be represented in the DEM (Fig.5 left). Since the calculated V doesn’t contain the volume under the water surface  $V_0$  (Fig.5 right), the corrected V for each water level is calculated by adding  $V_0$  on the calculated V, where  $V_0$  is given as the difference calculated V and observed V at high water level (in this study, observed V at high water level is obtained World Register of Dams (2)).

##### c) Identification of parameters a, b

The A-V relation for the reservoir is defined by the fitting of eq.(1) with the discrete pair of A and V obtained in previous sections. The parameters a and b in eq.(1) are estimated by the least square method.

Fig.6 shows A-V relation of the Yagisawa-reservoir, which is identified by the proposed method and DEM. The A-V relation of the Yagisawa-reservoir is obtained as follow;

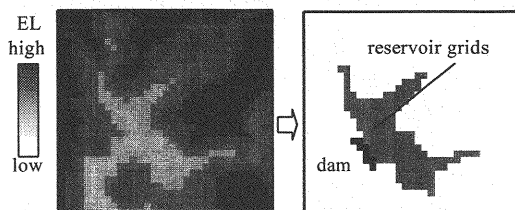


Fig.4 "reservoir grids" on DEM

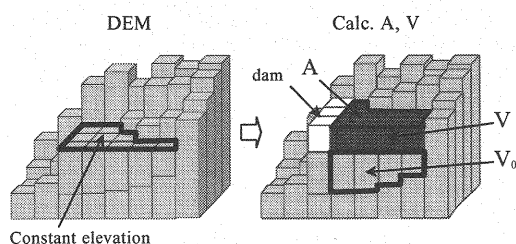


Fig.5 calculating A, V from DEM

$$V = 18.93 \cdot A^{1.49} \quad (A: \text{km}^2, V: 10^6 \text{m}^3)$$

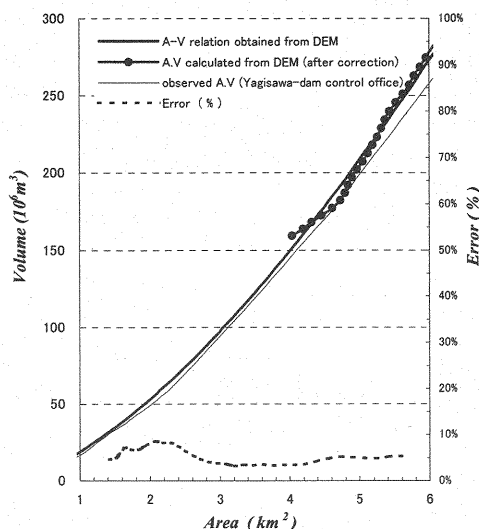


Fig.6 A-V relation for Yagisawa-reservoir

To verify the accuracy of eq.(5), the observed A-V relation is also plotted in Fig.6, where the observed A-V relation was provided by Yagisawa-dam Management Office on the basis of the contour map that was drawn before the dam was constructed. It showed a close agreement between eq.(5) and the observed A-V relation, although some discrepancies are found for higher water level. The relative error of the estimated A-V relation (eq.(5)) as compared with the observed one is calculated for every water level (every 1m) from the lowest one to the high flood water level (i.e. the range of possible change of water level due to reservoir operation). The average relative error is +5.2%, and the maximum one is +8.5%.

### ESTIMATION OF THE VOLUME OF WATER STORAGE

#### Extraction of the area of water surface (A) from satellite images

The following methods are used for extraction of the area of water surface (A).

##### a) Extracting from Visible and Near Infrared images

The detection of water surface in Visible and Near Infrared images (VIS/NIR images) are performed by combining both the image processing techniques (region growing algorithm (10)) and image interpretation (called as "quasi-automated method"). For the region growing algorithm spectral distance, which is the distance in n-dimensional feature space (11) and implies degree of similarity, is used to select pixels that have similar spectral properties as pixel of interest. The pixels within a certain spectral distance, which is given as the similarity threshold, are assumed to have similar spectral properties. Starting from the pixel in question on the water surface, similar pixels are selected from neighboring pixels and merged into same group. The processing of this integration is repeated until no similar pixels can be found from adjacent pixels. Then, the area of water surface is extracted from the images as a group of continuously linked pixels.

Fig.7 shows the extracted area of water surface (A) for several thresholds of spectral distance from ADEOS/AVNIR-M (Jun.16, 1997), in which A is calculated by multiplying the numbers of pixels and the area of a grid (16m x 16m). Moreover for SPOT/HRV-XS, A is calculated similarly, where the area of a grid is 20m x 20m. The area of water surface (A) is identified from these processed images, by referring to the shape of reservoir and contour lines on 1:25,000 scale topography map. Fig.9-1 shows the examples of extracted area of water surface from VIS/NIR images.

### b) Extracting from SAR images

Since a flat plane like a water surface can be assumed to be smooth as compared with microwave, backscattering of microwave on water surface is much smaller than other land covers, and the brightness of water surface in SAR images became lower than neighboring ones (12).

#### (b-1) Extraction by image reading

In this method, the area of water surface is extracted on the basis of the visual observation of images. The image enhancement (contrast stretch) and histogram equalization process are applied for original SAR images to facilitate the visual observation of water surface. The visual observation of water surface is

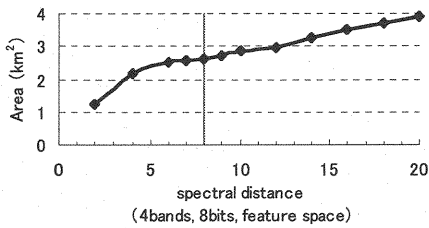


**Fig.7** Relationship between spectral distance and extracted area of water surface (ADEOS/AVNIR, Jan.16, 1997)

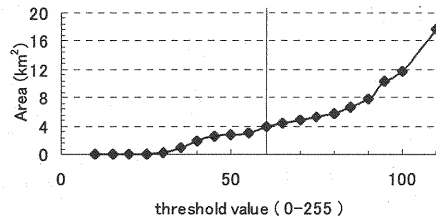


**Fig.8** Relationship between threshold value and extracted area of water surface (J-ERS1/SAR, Aug.7, 1994, quasi-automated method)

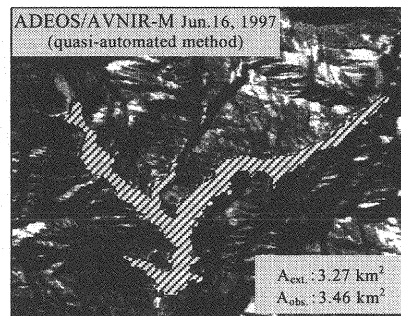
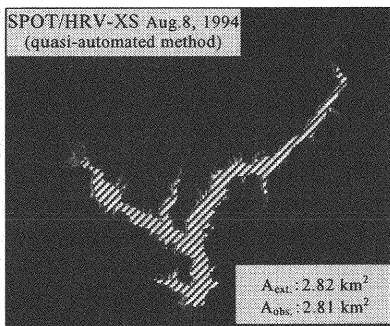


**Fig.9-1** Example of extracted area of water surface (VIS/NIR images)  
( $A_{ext}$  : extracted A from satellite images,  $A_{obs}$  : observed A by dam control office)

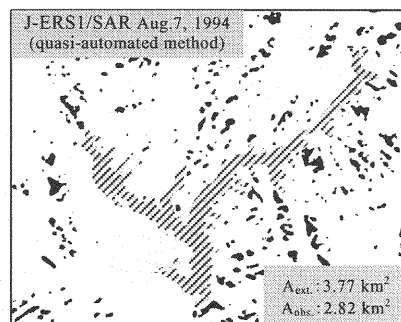
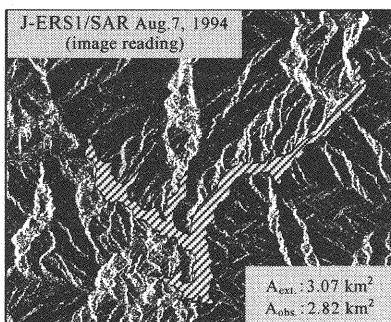


**Fig.9-2** Example of extracted area of water surface (SAR images)  
( $A_{ext}$  : extracted A from satellite images,  $A_{obs}$  : observed A by dam control office)

performed for the processed images by referring to the shape of reservoir and contour lines drawn on 1:25,000 scale topography map. The area of water surface (A) is calculated by multiplying the numbers of pixels in the area and area of a pixel ( $12.5\text{m} \times 12.5\text{m}$ ).

(b-2) Extraction by quasi-automated method

In addition to processes stated above, spatial filtering by  $3 \times 3$  smoothing filter is applied for the images to eliminate speckle noise. All pixels in processed images are classified into 2 categories (water surface and others) according to a certain threshold value. This process is referred to as “binarization”, and performed for several thresholds. For binarized images, a  $7 \times 7$  majority filter is applied to remove the isolated pixel of water surface, where majority filter changes the category of the pixel in question (water or others) into the predominant one within the surrounding  $7 \times 7$  pixels. From these processed images, the area of water surface (A) is identified, by referring to the shape of reservoir and contour lines on 1:25,000 scale topography map. Fig.8 shows the area of water surface (A) extracted for several thresholds. Furthermore, some corrections were made by means of a hand operator (e.g. the removal of the excess area of water surface which was found in higher regions than other water surface areas). Fig.9-2 shows an example of an extracted area from SAR images.

### Estimation of the volume of water storage

Using A-V relation in eq.(5), the volume of water storage (V) is estimated from the area of water surface (A) observed by satellite images. Table2 and Fig.10 show the results of estimation for the Yagisawa-reservoir. The accuracy of these estimates is evaluated by comparing the estimated V and observed ones provided by Yagisawa-dam Management Office.

The proposed method is applicable in that it can capture the trend of increase or decrease of water storage in the reservoir, although the estimated volume of water storage did not show a very satisfactory agreement with observed values. The comparison of various kinds of estimates, which are obtained from different satellite images and methods ((a), (b-1) and (b-2)), indicates that the quasi-automated method using SAR images (b-1) has a tendency to overestimate the storage. In this application, the relative error of (a), (b-1) and (b-2) are ranging from  $-25.4\%$  to  $7.6\%$ ,  $-5.5\%$  to  $60.2\%$ , and  $-10.4\%$  to  $18.2\%$ , and average of the absolute value of these relative error are  $8.3\%$ ,  $8.2\%$  and  $19.7\%$  respectively.

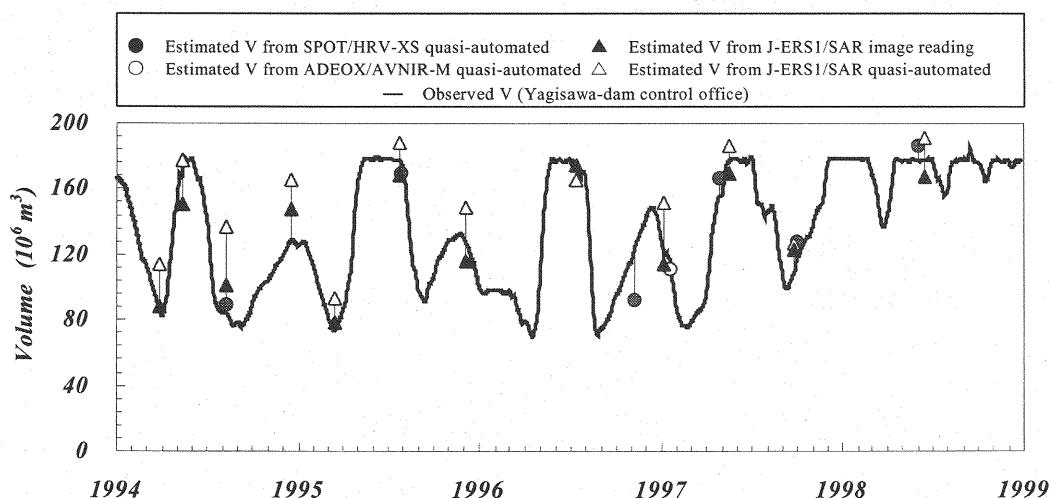
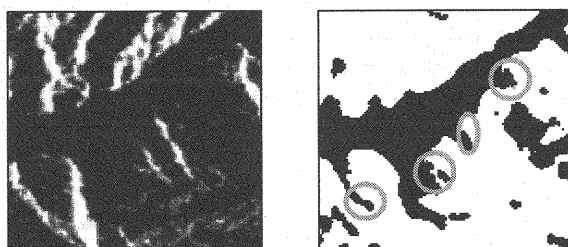


Fig.10 Result of estimation for the volume of water storage for Yagisawa-reservoir

**Table2** Estimation error of the volume of water storage for Yagisawa-reservoir  
(Error is absolute value of the relative error for the volume of water storage)

method		Number of used image	Error	
			average	maxmam
a	VIS/NIR (quasi-automated)	7	8.9%	25.4%
b-1	SAR (image reading)	12	8.6%	18.2%
b-2	SAR (quasi-automated)	12	19.7%	60.2%



**Fig.11** Example of misclassified area of water surface  
(left : SAR images, right : extracted water surface  
(quasi-automated method)) (J-ERS1/SAR,Aug.7,1994)

#### Analysis on the estimation error

The causes of error in the proposed algorithm can be separated into two parts: error of modeled A-V relation and error in the extraction of water surface. As shown in Fig.6, the error in the obtained A-V relation (eq.(5)) is not so large in comparison with the error of the estimated water storage. Thus, in case of this application, major problems can be ascribed to extraction methods of the water surface from satellite images. The conceivable factors of the error are discussed below.

##### a) Error from Visible and Near Infrared images

One of the factors that accounts for this is that partial area in the reservoir has different spectral features for VIS/NIR bands from the water surface (e.g. icy water surface), and could not be extracted by region growing algorithm. For example, an icy surface was found at the upper stream of the reservoir and aside the edge of water surface in ADEOS/AVNIR-M image (Jan.16, 1997). If the edge of the water surface (i.e. pixels next to water surface) is assumed to be an icy surface, the total icy area in the reservoir is approximately 0.63 km<sup>2</sup>, which is corresponding to 18% of the observed area of water surface. By adding it to the area of water surface, the relative error of storage volume estimation is improved to -5%.

The selection of optimal threshold is also considered to be a problem in the application of region growing algorithm to extract water surface. In case of ADEOS/AVNIR-M (Jan.16, 1997), the change of water surface caused by alteration of threshold is 0.08km<sup>2</sup> to 0.21km<sup>2</sup> and these correspond to 2% and 6% of the area of water surface, even if the change of threshold is only +1 or +2 from the optimal value used in this study.

##### b) Error from SAR images

The shaded area on mountainous topography is also thought to have a significant influence on extracting the area of water surface. As stated previously, backscattering of the microwave on the water surface is much smaller than other land covers, and the brightness of water surface in SAR images became lower than neighboring ones. However, the area other than water surface also gives lower backscattering depending upon the direction and incident angle of microwave beam, or the inclination and aspect of land surface. For this reason, the area of radar shadow or boundary of slope and water surface give small backscattering coefficients ( $\sigma_0$ ), and tend to misclassified as water surface (Fig.11).



In this application, ranges of relative errors of the extracted A from SAR images (total 12 scenes) are from -6.8% to 33.5% for quasi-automated method (b-1), from -9.8% to 8.9% for image reading (b-2). The average of these error of A are 10.0% for quasi-automated method (b-1), 6.0% for image reading method (b-2), and corresponding to 16% and 8.4% error of the amount of storage of water.

## CONCLUSIONS

In this study, an algorithm for estimating the storage of water in reservoirs from DEM and satellite images is proposed. This algorithm is able to estimate water storage in reservoirs from satellite data and DEM, and can be applied to other regions in the world. The proposed algorithm is applied for the Yagisawa-reservoir to evaluate its applicability. Although the estimated water storage does not yet satisfactorily agree with the observed one in some cases (especially in the case of quasi-automated method using SAR images), the possibility of estimating the storage volume by this method is promised. For practical use of this algorithm, we need to improve the accuracy of extracting area of water surface from satellite images, and to investigate the influence of backwater area in large reservoirs.

## ACKNOWLEDGEMENTS

Data on the Yagisawa-reservoir used in this study is supplied by Yagisawa-dam Management Office, Water Resources Development Public Corporation. And satellite images are supplied by National Space Development Agency of Japan (NASDA). The authors would like to acknowledge these organizations.

## REFERENCES

1. Vorosmarty et al : The Storage and Aging of Continental Runoff in Large Reservoir Systems of the World, *Ambio* ,Vol.26,No.4, pp. 210-219, 1996
2. ICOLD : World register of Dams. International Commission on Large Dams, 1998.
3. ICOLD : World register of Dams. International Commission on Large Dams, 1984,1988.
4. Rikimaru et al : Comparative study about ability of extracting water surface from RADARSAT SAR both Standard mode and Scan SAR Narrow mode, proceeding of the 26th RSSJ annual meeting, pp.409-410, 1999
5. Mutuda et al : Basic study about the method to extract changes of area of surface water by using plural SAR data, the proceeding of the 52th JSCE annual meeting, 2, pp.388-389, 1997
6. Takeuchi K : On the scale diseconomy of large reservoirs inland occupation, IAHS Publication no.240, pp. 519-527, 1997
7. Takeuchi K et al : Sustainable Reservoir Development and Management, IAHS Publication no.251, pp. 4-9, 1998
8. The Japan dam foundation : Yearbook of dams 1990, 1996
9. Magome et al : Development of a method for calculation water storage in reservoirs by using DEM, the proceeding of the 54th JSCE annual meeting, 2, pp.604-605, 1999
10. Hideyuki T. : Computer image processing guide, Soukei-shuppan, pp.128-132, 1985
11. ERDAS, Inc. : ERDAS Field Guide, forth edition, pp.456, 1997
12. JSPRS : Handbook of SAR images, pp.83-88, 1998

(Received August 20, 2001 ; revised February 22, 2002)